Chapter 1

Localized Surface Plasmon Resonance (LSPR)-Coupled Fiber-Optic Nanoprobe for the Detection of Protein Biomarkers

Jianjun Wei, Zheng Zeng, and Yongbin Lin

Abstract

Here is presented a miniaturized, fiber-optic (FO) nanoprobe biosensor based on the localized surface plasmon resonance (LSPR) at the reusable dielectric-metallic hybrid interface with a robust, gold nano-disk array at the fiber end facet. The nanodisk array is directly fabricated using electron beam lithography (EBL) and metal lift-off process. The free prostate-specific antigen (f-PSA) has been detected with a mouse anti-human prostate-specific antigen (PSA) monoclonal antibody (mAb) as a specific receptor linked with a self-assembled monolayer (SAM) at the LSPR-FO facet surfaces. Experimental investigation and data analysis found near field refractive index (RI) sensitivity at ~226 nm/RIU with the LSPR-FO nanoprobe, and demonstrated the lowest limit of detection (LOD) at 100 fg/mL (~3 fM) of f-PSA in PBS solutions. The SAM shows insignificant nonspecific binding to the target biomarkers in the solution. The control experimentation using 5 mg/mL bovine serum albumin in PBS and nonspecific surface test shows the excellent specificity and selectivity in the detection of f-PSA in PBS. These results indicate important progress toward a miniaturized, multifunctional fiber-optic technology that integrates informational communication and sensing function for developing a high-performance, label-free, point-of-care (POC) device.

Key words Fiber optics, Protein biomarker biosensors, Nanofabrication, Au nanodisk array, Localized surface plasmon resonance (LSPR), Signal transduction

1 Introduction

Recent advances of biomarker detection have been made in optical fluorescence [1], light scattering [2], surface enhanced Raman spectroscopy (SERS) [3], electrochemical [4], functional quartz crystal microbalance [5], microcantilevers [6], and surface plasmon resonance (SPR) imaging [7] sensors. Harnessing the advances in biological ligand interactions, the fiber-optic (FO) technology incorporating localized surface plasmon resonance (LSPR) nanoprobe sensing may provide an alternative tool for effective biomarker diagnosis via a compact, label-free format that does not require a

Avraham Rasooly and Ben Prickril (eds.), *Biosensors and Biodetection: Methods and Protocols Volume 1: Optical-Based Detectors*, Methods in Molecular Biology, vol. 1571, DOI 10.1007/978-1-4939-6848-0_1,

dedicated laboratory facility or highly trained personnel. Furthermore, there is a need to develop advanced LSPR-FO biosensors that may avoid the use of bulky optics and high-precision mechanics for angular or wavelength interrogation of metal films in contact with analytes, and provide high-performance, e.g., enhanced stability and high RI sensitivity, and overcome unwanted doping or weak adhesion.

Surface plasmon resonance (SPR) is the resonance oscillation of conduction electrons at the interface between a negative and a positive permittivity material excited by an electromagnetic radiation, e.g., light. The surface plasmon polaritons (SPPs) launched upon the radiation can be propagating along the metal-dielectric interface and decay evanescently at the normal direction for a flat surface. Surface plasmons [8] (SPs) are very sensitive to the near surface refractive index (RI) changes and well suited to the detection of surface-binding events. The basic methodology of SPR sensing is based on the Kretschmann configuration (Fig. 1) where a prism is used for the light-SP coupling at the surface of a thin metal film. The probe light undergoes total internal reflection on the inner surface of the prism. At a defined SPR angle, an evanescent light field travels through the thin gold film and excites SPs at the metal-dielectric interface, reducing the intensity of the reflected light at the resonance wavelength or changing the phase of the incident light. The intensities of scattered and transmitted light fields are used to determine the thickness and/or dielectric constant of the coating [9]. The control variables for SPR sensor applications, i.e., the wavelength of incident light, the thickness of the metal film, the physical and optical properties of the prism, and the RI of the medium near the metallic interface have been well studied [10]. However, the advantages of averaging over a large surface area and the challenges of miniaturizing the optics limit the integration of SPR-based sensing.

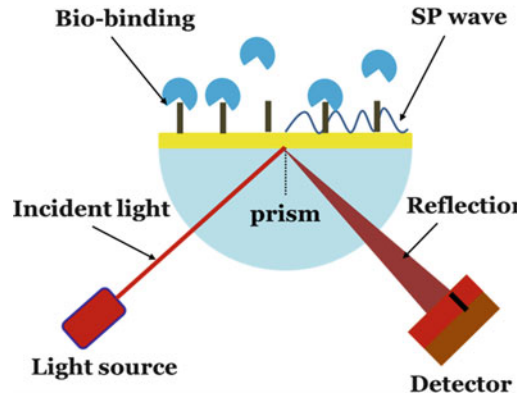

Fig. 1 A conventional surface plasmon resonance (SPR) configuration and setup for biological sensing

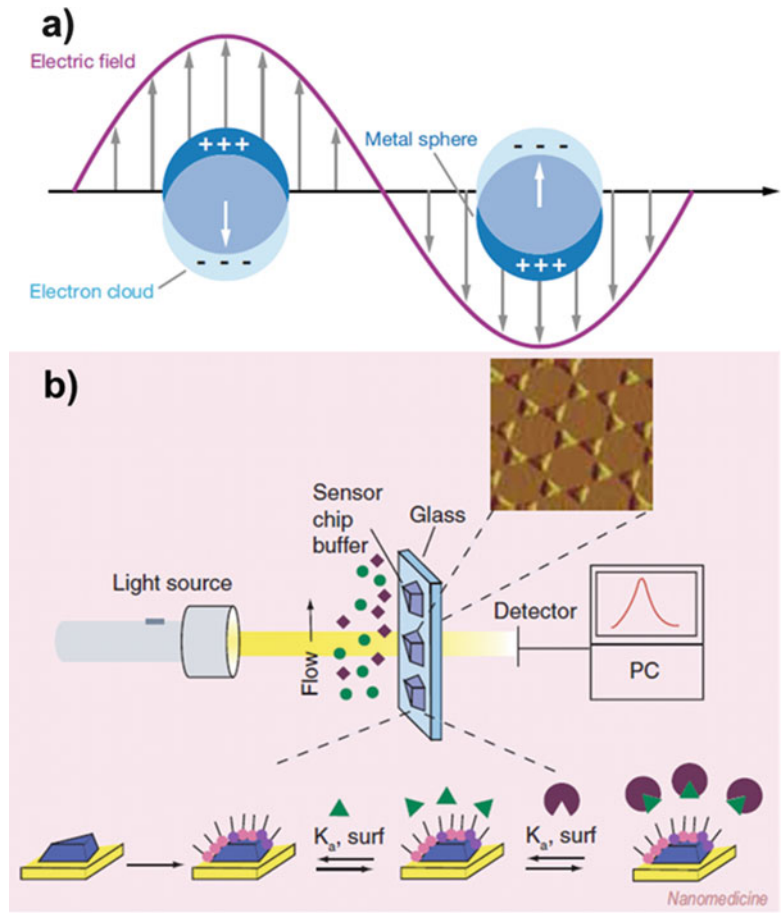

Fig. 2 Schematic diagrams illustrating (**a**) a localized surface plasmon [18], (**b**) a configuration of representative experimental setup and procedure for LSPR sensing [19]

LSPR is caused by resonant surface plasmons localized in nanoscale systems when light interacts with particles much smaller than the incident wavelength (Fig. 2a). Similar to the SPR, the LSPR is sensitive to changes in the local dielectric environment near the nanoparticle surfaces. Usually, the sense changes are measured in the local environment through an LSPR wavelength shift of the scattering light via reflection or transmission (Fig. 2b). Nanoscale LSPR makes possible for the development of a portable device for point-of-care (POC) detection regarding its requirements, such as robust to handle, small volume sample, and little to no sample pretreatment, label-free and rapid response time, and compact size.

Incorporation of the LSPR to fiber optics (FO) offers a few advantages in terms of avoiding the use of bulky optics and high-precision mechanics for angular or wavelength interrogation of

metal films in contact with analytes, including immobilization of Au or Ag nanoparticles (NPs) to optical fiber probes for LSPR detection [11, 12]. It may allow realizing an optical communication and analytical tool for a wide spectrum of applications. However, more controllable and stable LSPR nanoscale systems for fiber optic integration are desirable to develop robust, reliable, portable LSPR biosensors.

In this work, the progress of developing a miniaturized LSPR-FO probe and demonstration of sensitive, label-free detection of a protein cancer biomarker, free prostate-specific antigen (f-PSA) are reported, which involves three major steps: (1) a low-cost lift-off process adapted to fabricate gold nanodisk arrays at the end of tip-facet, providing a very stable, robust, and clean LSPR fiber tip probe, (2) the probe was functionalized via a facile self-assembled monolayer (SAM) of alkanethiolates on the gold nanodisk array to attach a capture ligand, anti-PSA antibody, as a selective immunoassay for the detection of the f-PSA, (3) the FO-based sensing technology was used as a powerful analytical tool by integrating the LSPR nanoprobe to communicative fiber optics. The sensing principle and configuration of the LSPR nanoprobe is shown in Fig. 3. The white light guided in the optical fiber using as incident light to the gold nanodisk arrays at the end of the fiber tip surface for excitation of the LSPR. The reflectance of the light scattering from the nanodisk arrays was recorded before and after the biological binding. The correlation of the changes of reflectance spectra to the binding of the analytes to the nanodisk arrays, corresponding to the analyte concentrations in samples, was established for detection. The reported label-free LSPR fiber biosensor may allow an alternative approach for direct discrimination of the

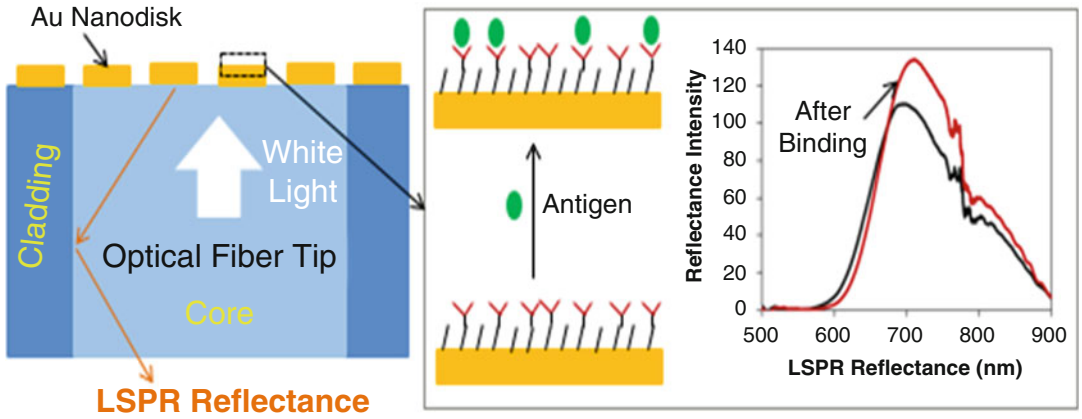

Fig. 3 A diagram illustrating the principle of LSPR coupling on fiber optic probe for biosensing. The nanodisk arrays are fabricated on optical fiber tip end. The LSPR reflectance is recorded with a white incident light guided in the fiber

cancer biomarkers, and potentially developing a miniaturized, point-of-care (POC) device for early disease diagnosis.

This work suggests that: (1) as an emerging technology, the LSPR-FO sensor has ultra-high sensitivity in molecular adsorption detection; (2) the LSPR Au nano-array fabricated at the end facet of the fiber tip for sensing is very robust and reusable; (3) the primary resonant wavelength can be tuned to a desired range (e.g., NIR) by tailoring the nano-array structure to enhance the sensitivity; (4) tailored surface functionalization harnessing the advances in biological ligand interactions (e.g., immunoassays) enables signal amplification and a label-free, selective detection; and (5) the target molecules are immobilized by dipping the fiber-optic probe in sample/reagent solution, contrary to pouring of sample solution in conventional methods (ELISA, Electrochemiluminscence, Radioimmunoassay-RIA), resulting in drastic reduction of the amount of sample/reagents needed and decreases the washing time of probes.

2 Materials and Equipment

1. Single-mode optical fiber for 633 nm wavelength was purchased from Newport Corporation.
2. Electron beam resist (ZEP-520A), thinner (ZEP-A), developer (ZED-N50), resist remover (ZEDMAC) were purchased from ZEON Corporation, Japan, and used without further purification.
3. 11-Mecaptoundecanoic acid (HSC10COOH, 99%), 8-Mercapto-1-Octanol (HSC8OH, 98%), *N*-(3-Dimethylaminopropyl)-*N*′-ethylcarbodiimide hydrochloride (EDC), *N*-Hydroxysuccinimide (NHS), and glycine were purchased from Sigma-Aldrich (Milwaukee, WI) and used without further purification.
4. Mouse anti-human PSA monoclonal antibody (capture mAb), human free-PSA, and ELISA kits for CA125 were obtained from Anogen-YES Biotech Laboratories Ltd. (Mississauga, Canada).
5. The 5 ng/mL free-PSA standard solution was used for preparation of free-PSA solutions with lower concentrations obtained using sample dilutant provided in the ELISA kit. The 5 ng/mL free-PSA standard solution was prepared in a protein matrix solution according to the World Health Organization (WHO) standard [13] by the vendor.
6. Chrome etchant was obtained from Microchem GmbH, Germany.

7. The fiber clamp for hoisting fiber for vibration was obtained from Newport Corporation, CA, USA.
8. Ultra clean convection oven (Ultra-clean 100) was obtained from Thermo Fisher Scientific, OH, USA.
9. Nano pattern generation system (NPGS) was obtained from JC Nabity Lithography Systems, MT, USA.
10. Field emission scanning electron microscope (FESEM) was a LEO 1550 model.
11. Three cathode vacuum sputter system (Denton Discovery-18 Sputter System) was obtained from Denton Vacuum LLC, NJ, USA.
12. Vacuum thermal evaporate system was donated to University of Alabama in Huntsville by US Army.
13. Reactive Ion Etching (RIE) system (Plasma-Therm 790) was obtained from Plasma-Therm, FL, USA.
14. Optical fiber coupled Tungsten Halogen light source (LS-1) was obtained from Ocean Optics, FL, USA.
15. Mini-spectrometer (USB2000-VIS-NIR) was obtained from Ocean Optics, FL, USA.
16. 2 × 2 Single-mode fiber optic couplers for 633 nm wavelength were obtained from Newport Corporation, CA, USA.

3 Methods

3.1 Fabrication of LSPR-FO Nanoprobe

1. Typical semiconductor fabrication technologies [14, 15] with lift-off method are utilized in the fabrication development for Au nanostructures on fiber end face, as schematically illustrated in Fig. 4. There are four main technological steps: (1) deposition of positive electron beam resist (ZEP520A, Zeon Chemicals, Japan) on the fiber end face with uniform thickness (Fig. 4a–c), (2) nano-patterning on the E-beam resist using EBL method (Fig. 4d), (3) vacuum deposition of functional metallic materials over the e-beam resist using cleanroom

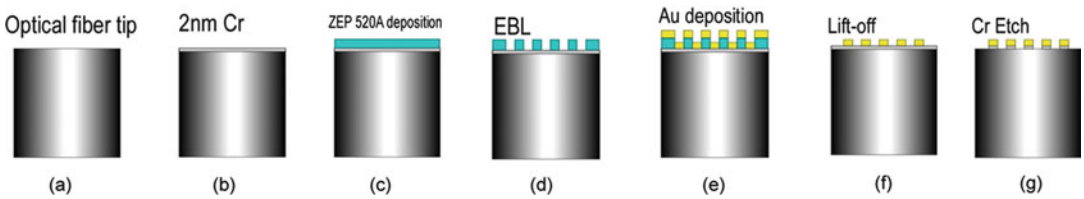

Fig. 4 A schematic flow-chart displays the fabrication procedure for nanodisk arrays at the optical fiber end facet. (**a**) optical fiber tip, (**b**) 2 nm Cr deposition, (**c**) resist deposition, (**d**) EBL process, (**e**) gold film deposition, (**f**) lift-off process, (**g**) Cr etch to get the nanodisk arrays

thermal evaporation (Fig. 4e), and (4) nano-pattern transfer using standard liftoff method (Fig. 4f, g).

2. An optical fiber for single-mode wavelength of 633 nm is employed in this work, which has a core diameter of 4 μm, a cladding diameter of 125 μm, and a polymer buffer coating diameter of 250 μm (Fig. 4a). Compared to standard optical fiber operated at single-mode wavelength of 1310 nm, the advantage of using this small core fiber is that it provides more spectral stability in the wavelength ranges of 600–750 nm, in which locate the resonance peak of our fabricated fiber tip LSPR sensors. Small core size also means higher fabrication yield and less nanoparticles involved in the sensing, thus requires smaller amount of target samples.
3. The preparation of optical fiber tip includes stripping off the polymer buffer layer 4 cm from the end and cleaving the end face with a fiber cleaver, followed by cleaning with acetone and isopropyl alcohol (IPA) rinse for 5 min.
4. Two nanometers of Cr film is firstly deposited on the fiber end face using the vacuum sputtering method [16] to provide a conductive layer for the e-beam resist in the EBL process (Fig. 4b).
5. A simple and unique wet resist coating method called "dip and vibration" technique has been developed in a nanofabrication lab to deposit e-beam resist on the optical fiber tip (Fig. 4c), and its procedure is schematically represented in Fig. 5. The optical fiber is dipped into the diluted e-beam resist (ZEP520A diluted with ZEP thinner at a ratio of 1:3) for 10 s (Fig. 5a). Then, it is removed from the resist and hoisted into a vertically upward position using a Newport fiber clamp, with ~15 mm of fiber tip outside the clamp at the top (Fig. 5b, c).

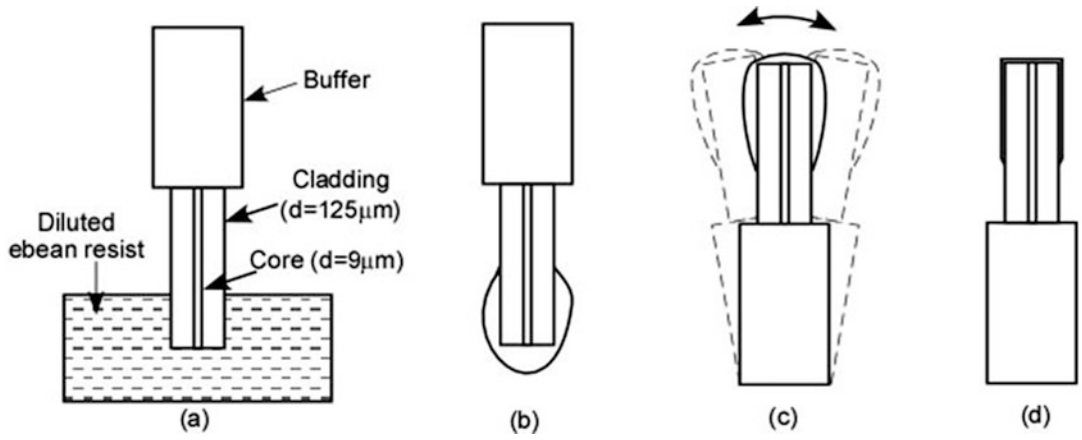

Fig. 5 Illustrations of the procedure called "dip and vibration" technique, (**a**) dip in the diluted e-beam resist, (**b**) after dip, (**c**) vibration, and (**d**) after bake

The fiber tip is then vibrated manually by pulling the fiber tip to one side and then releasing to get rid of excessive resist by means of cantilever beam free vibration. The vibration frequency and strength is controlled by the length of fiber tip outside the fiber clamp and the initial displacement of the fiber tip. The thickness of resist on the optical fiber tip is dependent on the ZEP dilution ratio and vibration strength. The iterative method is used to optimize the vibration process. The initial fiber tip displacement for the vibration is 2–5 mm, and the fiber tip length is 15–25 mm. The ZEP dilution ratio used is from 20% to 40%, diluted in ZEP thinner. The resulted e-beam resist layer thickness on the fiber tip is 100–200 nm, measured by SEM observation. The fiber tip is held vertically upward and baked in a 120° C oven for 60 min (Fig. 5d).

6. The EBL process based on the Nano Pattern Generation System (NPGS) and a field emission scanning electron microscope (FESEM) is used to create nanodot array pattern on the e-beam resist on the fiber end face (Fig. 4d). A Newport fiber clamp is used to hold the fiber vertically on the translation stage in the SEM chamber. The EBL voltage is 30 kV and the exposure dose is 70 $\mu C/cm^2$. The fiber tip is developed by dipping in resist developer (ZEP N50) for 1 min. The fiber tip is then rinsed in DI water and baked in the 120° C oven for 10 min for dehydration.
7. An oxygen plasma descum procedure in a reactive ion etcher (RIE, 25 watts power for 3 min) is used to remove the thin residual layers of photoresist following the photoresist development step (*see* **Note 1**).
8. The deposition of 40 nm Au overlay over the patterned area is carried out by using the standard thermal evaporation coating technique (Fig. 4e). The 2 nm Cr layer previously deposited as a conductive layer for the EBL process is now served as an adhesive layer for Au overlay. To lift off the e-beam resist, the fiber tip is dipped in the ZEP remover for 10 min, followed by a 1-min ultrasonic bath to assist the lift-off process (Fig. 4f). The fiber tip is rinsed in DI water and checked under an optical microscope to make sure that the resist layer on the fiber end face has been removed (*see* **Note 2**).
9. The fiber tip is dipped into the Cr remover solution for 30 s to remove the Cr layer that is not covered by the Au nanoparticles (Fig. 4g). The fiber tip is rinsed again in DI water and baked in the 120 °C oven for 10 min for dehydration. Figure 6 shows the scanning electron micrographs of a gold nanodisks array on an optical fiber tip end facet.
10. Finally, the Au nanodisk array on fiber end face is annealed at 530 °C for 5 min and ready for next usage (*see* **Note 3**).

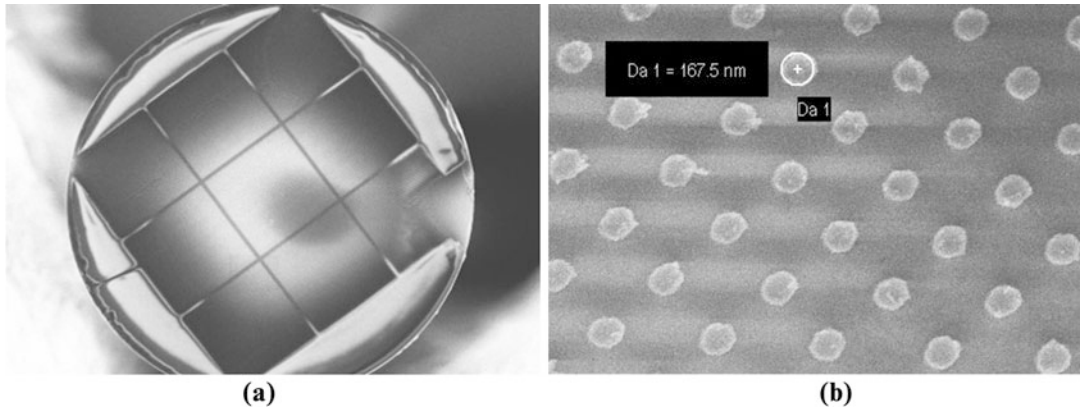

Fig. 6 Images of (**a**) overview of the optical fiber tip end, (**b**) SEM images of gold nanodisk arrays on the optical fiber facet after the lift-off process

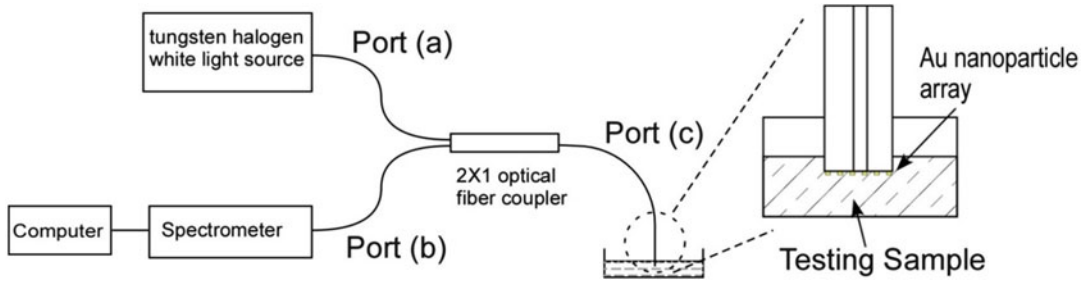

Fig. 7 A schematic diagram illustrating optical setup for the fiber tip LSPR sensor based on reflection spectrum measurement

3.2 Optical Measurement

1. In this optical setup (Fig. 7), a 2 × 1 single-mode optical fiber coupler for 633 nm wavelength is used, which has three light connection ports. In Fig. 7, port (a) and port (b) are two connections on one side of optical fiber coupler, and port (c) is connection on the opposite side. Port (a) is connected to the tungsten halogen white light source; port (b) is connected to a mini-spectrometer; and port (c) is connected to the LSPR-FO probe using a fusion splicer. The white light (450–950 nm) is launched from port (a), propagated to port (c), and reflected from the end facet with the Au nanodisks arrays. The reflection light propagated to port (b), where the spectrum of the reflection light is measured by the mini-spectrometer, which is connected to a computer for data acquisition and processing. Figure 8 shows the photograph of the Optical setup for the fiber tip LSPR sensor based on reflection spectrum measurement.
2. During fiber optic LSPR detection, the light is launched and guided to the LSPR fiber tip facet. The light wave propagates along the core in the center of the optical fiber tip where the

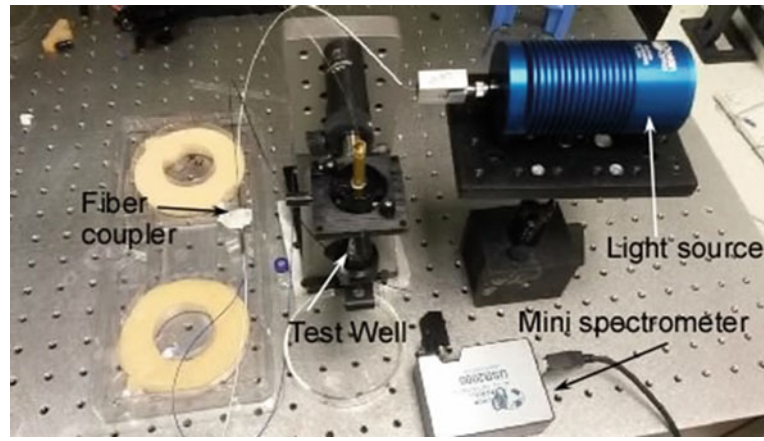

Fig. 8 Photograph of the optical components (optical fiber, fiber coupler, mini-spectrometer, light source) and setup for the fiber tip LSPR sensor. Computer connection to the mini spectrometer via USB cable is not shown

nanodisk array is located. The guided white light interacts with the Au nanodisk array and excites the localized surface plasmon giving raise to enhanced scattering around the resonance wavelength. The LSPR wavelength strongly depends on interface refractive properties [16]. The light reflected from the LSPR interface is guided in the fiber and propagated to the mini-spectrometer, and the spectrum of the reflected light is recorded as a function of wavelength. The detection of RI change at the interface is accomplished by observing the primary resonance peak shift in the spectrum.

3. Before starting the experiment, the sensor tip must be cleaned of any impurities or other contaminants. The sensor tip is rinsed with ethanol to clean the tip. A baseline wavelength is achieved if the sensor tip returns to this wavelength three times after being washed in deionized water. If the tip spectra do not return to this line, acetone and isopropyl alcohol (IPA) dip for 5 min may be used to further clean the tip of lingering impurities.
4. In order to get the LSPR spectrum response due to Au nanostructures on the fiber end facet, a reference spectrum and a dark spectrum need to be recorded. The reference spectrum is acquired without fiber LSPR probe on port (c), and the fiber end face of port (c) is perpendicularly cleaved. The dark spectrum is obtained by turning off both the tungsten halogen light source and room light. The measured reflection spectra (M_λ) of the fiber tip sensor probe is obtained by the equation:

$$M_\lambda = (S_\lambda - D_\lambda)/(R_\lambda - D_\lambda) \times 100\ \%\ ,$$

where S_λ is the sample intensity, D_λ is the dark intensity, and R_λ is the reference intensity at wavelength λ (the intensity defines as photon counts).

3.3 LSPR-FO Nanoprobe Sensitivity Characterization

1. The nanoprobe sensitivity is used to determine if the sensor tip in experimentation would be sensitive enough to determine small wavelength shifts accurately.
2. The solvents used in determining the bulk RI sensitivity of the LSPR tip are acetone, methanol, ethanol, isopropyl alcohol, and water of different RIs.
3. The LSPR-FO nanoprobe is dipped in the various solvents, and the spectra of the reflected light were recorded, respectively, as shown in Fig. 9a (*see* **Note 4**).
4. To determine the peak wavelength in the LSPR reflection spectrum, a Matlab program was created to fit the data to an eighth-order polynomial function over a range of 80 nm [17], centered at the wavelength of maximum reflection in the raw data.
5. The calculated LSPR wavelength red shifted as the RI of the solvent increased. A linear relationship between the LSPR peak wavelength and the bulk RI of the medium is obtained (Fig. 9b black dots), with the sensitivity of 226 nm/RIU (RIU, refractive index unit) used in this study.
6. The light intensity-based RI sensitivity is investigated as well (Fig. 9b red diamonds). The return light intensities at the LSPR peak wavelength are plotted against the bulk RI of the media. The LSPR peak intensity is seen to be linearly proportional to the RI, and the gradient of the line is 123 per RIU. The return light intensity of a single-wavelength laser can be used as a probing light for the refractive index change due to

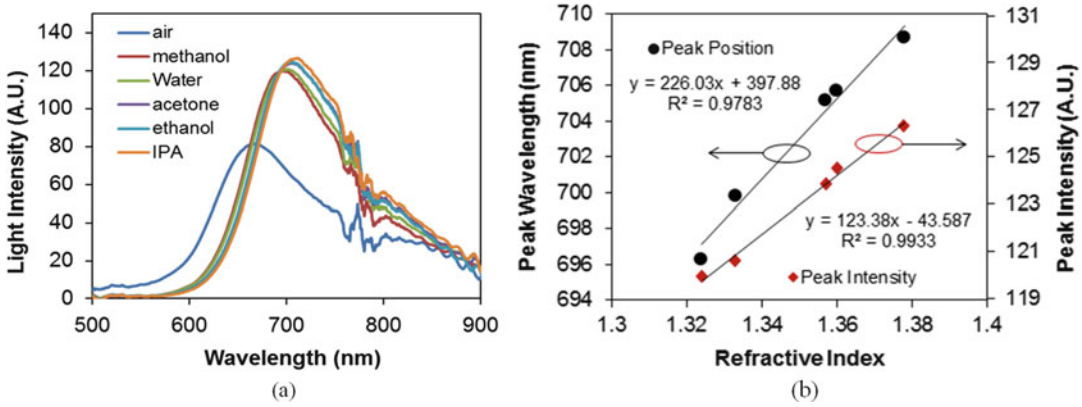

Fig. 9 Sensitivity measurements of the LSPR-FO nanoprobe. (**a**) Measured reflectance spectra for the LSPR-FO probe in various solvents of different refractive index. (**b**) Correlation of the LSPR peak wavelengths (*left axis*) and LSPR peak intensity (*right axis*) with the refractive index (RI) of the solvents, the linear fit of the changes vs. the RI gives the sensing sensitivity. In the inset equation, *x* and *y* represent the values of *x* and *y* axis. R^2 is the coefficient of determination in the linear fitting

biochemistry binding events, and thus eliminate the need for a broadband light source and optical spectrometer for an LSPR biosensing.

3.4 Functionalization of the LSPR-FO Nanoprobe

1. To achieve the immobilization of mAb at the LSPR-FO sensor surface, the first step is to incubate a cleaned gold nanodisck fiber tip in a mixture of 1 mM $HS(CH_2)_{10}COOH$ and $HS(CH_2)_8OH$ with mole ratio 1:5 in absolute ethanol solution for 1 h. A mixed self-assembled monolayer is formed at the gold nanodisck surfaces.
2. The self-assembled monolayer (SAM) tethered with carboxylic acid groups then is activated by incubation in a pH 7.0, 10 mM phosphate buffer solution containing 0.5 mM of EDC/NHS, respectively, for 1 h.
3. The activated SAM is rinsed with the distilled water and immediately moved to a freshly prepared 10 mM PBS containing 10 μg/mL of the detector mAb for 1 h incubation.
4. The fiber probe is finally rinsed with the PBS and followed by dipping in a 0.2 M glycine PBS solution for 10 min to deactivate the remaining active sites at the SAM.

3.5 Detection of f-PSA Biomarker

1. During the experiments, PBS (containing 0.05% tween-20) is used as a running buffer to help minimize the nonspecific adsorption of f-PSA at the fiber tips.
2. In order to test binding of PSA to the anti-PSA mAb modified surfaces, five tenfold-dilutions of a 5 ng/mL concentration of f-PSA are prepared in PBS solution for the desired concentrations (i.e., 5 ng/mL, 0.5 ng/mL, 0.05 ng/mL, 5 pg/mL, 0.5 pg/mL, 0.05 pg/mL). The sensor tip is placed in the f-PSA PBS for 10 min in the sequence at the lowest concentration of 50 fg/mL to measure the reflectance spectrum.
3. After each measurement, the fiber tip is rinsed thoroughly with DI water and dried in air. All spectra are obtained after the fiber tip was cleaned and dried in air. Figure 10a shows the representative reflectance spectra of f-PSA detection sensing various f-PSA concentrations from 0 to 0.5 ng/mL.
4. Figure 10b shows the dependence of the wavelength peak shift on the f-PSA concentration. The peak shift for each point is obtained by averaging three measurements. A wavelength shift of twice the largest standard deviation (1.2 nm) is used to determine LOD of the fiber LSPR sensors, which corresponds to 100 fg/mL of f-PSA in PBS solution.
5. Control experiments have been designed and carried out to evaluate the specificity/selectivity of the immunoassay using the LSPR-FO devices. Specifically, the binding between the detector mAb and bovine serum albumin (BSA), similar to

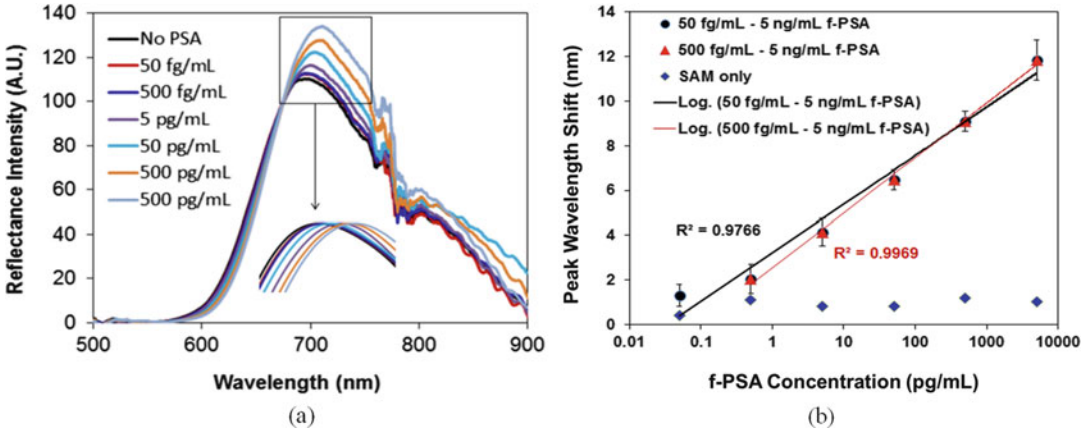

Fig. 10 Detection of protein biomarker. (**a**) The representative reflectance spectra of the anti-PSA mAb modified LSPR-FO nanoprobe in various concentrations of f-PSA (from 0 up to 0.5 ng/mL). Insert plot shows spectra normalized to peak intensity to show the LSPR reflectance peak shifts. (**b**) Correlation of f-PSA concentration to the reflectance light of resonance peak wavelength shift

human serum albumin, at concentrations of 5 mg/mL has been evaluated. Additionally, to evaluate the nonspecific binding to the SAM, the LSPR-FO devices modified only with the mix SAM of HSC10COOH and HSC8OH SAM without antibody attached are tested by following the f-PSA detection process, as shown in Fig. 10b (blue diamond markers).

4 Notes

1. The optional step after the oxygen descum is to dip the fiber tip in the chrome remover solution for 60 s to remove the thin Cr layer on the nanodisk area. This step will eliminate the Cr adhesion layer under the Au nanodisk, avoiding the undesired side effects of Cr layer under Au nanodisk in the LSPR sensing process, such as spectrum broadening and dephasing. However, this step will weaken the adhesion strength between the Au nanodisks and the fiber end glass substrate, and will reduce the reusability of the fiber LSPR probe.
2. If the lift-off process is not complete, ZEP remover and ultrasonic bath may be used to further lift off the e-beam resist.
3. The fiber probe is inserted horizontally into the oven through an access hole on the sidewall of a high-temperature oven. In order to protect the polymer buffer on the fiber, only 10–15 mm of fiber probe needs to be inside the oven.
4. Note that there is a noisy region in all spectra from ~760 to 800 nm, which is caused by the transmission minimum for the optical fiber coupler (single mode at 633 nm) in the same wavelength range.

Reference

1. Mukundan H et al (2009) Optimizing a waveguide-based sandwich immunoassay for tumor biomarkers: evaluating fluorescent labels and functional surfaces. Bioconjug Chem 20 (2):222–230
2. Liu X et al (2008) A one-step homogeneous immunoassay for cancer biomarker detection using gold nanoparticle probes coupled with dynamic light scattering. J Am Chem Soc 130 (9):2780–2782
3. Sekhar PK, Ramgir NS, Bhansali S (2008) Metal-decorated silica nanowires: an active surface-enhanced raman substrate for cancer biomarker detection. J Phys Chem C 112 (6):1729–1734
4. Mani V et al (2009) Ultrasensitive immunosensor for cancer biomarker proteins using gold nanoparticle film electrodes and multienzyme-particle amplification. ACS Nano 3 (3):585–594
5. Henne WA et al (2006) Detection of folate binding protein with enhanced sensitivity using a functionalized quartz crystal microbalance sensor. Anal Chem 78(14):4880–4884
6. Baker GA, Desikan R, Thundat T (2008) Label-free sugar detection using phenylboronic acid-functionalized piezoresistive microcantilevers. Anal Chem 80(13):4860–4865
7. Lee HJ, Nedelkov D, Corn RM (2006) Surface plasmon resonance imaging measurements of antibody arrays for the multiplexed detection of low molecular weight protein biomarkers. Anal Chem 78(18):6504–6510
8. Raether H (1988) Surface plasmons on smooth and rough surfaces and on gratings. Springer tracts in modern physics. Springer, Berlin
9. Leskova TA, Maradudin AA, Zierau W (2005) Surface plasmon polariton propagation near an index step. Optics Commun 249(1–3):23–35
10. Jung LS et al (1998) Quantitative interpretation of the response of surface plasmon resonance sensors to adsorbed films. Langmuir 14 (19):5636–5648
11. Mitsui K, Handa Y, Kajikawa K (2004) Optical fiber affinity biosensor based on localized surface plasmon resonance. Appl Phys Lett 85 (18):4231–4233
12. Chang T-C et al (2012) Using a fiber optic particle plasmon resonance biosensor to determine kinetic constants of antigen–antibody binding reaction. Anal Chem 85(1):245–250
13. 1985. http://apps.who.int/iris/bitstream/10665/38405/1/WHO_TRS_725.pdf.
14. Nishi Y, Doering R (2000) Handbook of semiconductor manufacturing technology. CRC Press, Boca Raton, FL
15. May GS, Spanos CJ (2006) Fundamentals of semiconductor manufacturing and process control. John Wiley & Sons, New York, NY
16. Obando LA, Booksh KS (1999) Tuning dynamic range and sensitivity of white-light, multimode, fiber-optic surface plasmon resonance sensors. Anal Chem 71(22):5116–5122
17. Wu H-J et al (2012) Membrane-protein binding measured with solution-phase plasmonic nanocube sensors. Nat Methods 9(12):1189–1191
18. Willets KA, Van Duyne RP (2007) Localized surface plasmon resonance spectroscopy and sensing. Annu Rev Phys Chem 58(1):267–297
19. Zhao J et al (2006) Localized surface plasmon resonance biosensors. Nanomedicine 1 (2):219–228